An Approach of Segregation in Modeling Continuous flow Tank Bioleach Systems

Athanasios Kotsiopoulos, Geoffrey S. Hansford, and Randhir Rawatlal
Dept. of Chemical Engineering, University of Cape Town, Rondebosch 7701, South Africa

DOI 10.1002/aic.11479
Published online April 9, 2008 in Wiley InterScience (www.interscience.wiley.com).

Published models apply particle size to predict bioleaching reactor performance. In this study mathematical models predicting the overall reaction rate of a bioleach reactor system are developed to establish which particle parameters are necessary to describe reactor performance. Since the intrinsic leaching rate is surface area dependent, the inlet particle size and residence time are model inputs. Three models, distinguished by the incorporation of age and/or size distributions, were developed from first principles through a segregation approach. Explicit dependence on the age distribution, allows the model extension to unsteady state behavior and imperfect mixing. The models are validated against pilot plant data for pyrite-arsenopyrite concentrates obtained from the Fairview Mine in South Africa. Simulation results indicate that only a model that considers both the particle age and size distribution is in good agreement with the data. © 2008 American Institute of Chemical Engineers *AIChE J,* 54: 1592–1599, 2008
Keywords: mathematical modeling, bioprocess engineering, reactor analysis, extraction, design (process simulation)

Introduction

Bioleaching of sulfide minerals is a process that has demonstrated its potential for the recovery of copper, gold, cobalt, and other base metals.[1,2] In heap leaching sulfide mineral stacks are irrigated with an acidic leach liquor and aerated at the base to facilitate mineral recovery. Although heap leaching is an effective bioleaching application that can process large volumes of minerals, it suffers from production and yield limitations due to process control inefficiencies.[1] This has led to an increased interest in the continuous analog, i.e. the continuous stirred tank bioleach reactor.[2] Contrary to heap leaching, the operating variables, namely, temperature, pH, and carbon dioxide transfer can, in tank bioleaching, be effectively controlled to obtain a higher degree of extraction.[1,3]

Tank bioleaching has been used for the recovery of gold from arsenic gold-bearing concentrates since 1984.[4] Subsequently, several large scale plants have been established with many patent operations arising (BIOX—Fairview, BacTech—Mintek, BioCop—BHP Billiton/Coldelco). One tool for improving the design, operation, and control of these processes is a dynamic reactor model.

To develop such a model from first principles, using pyrite as a model compound, the intrinsic kinetics of the reactions involved in the bioleaching process needs to be understood. A multistep process which includes the acid-ferric leaching and microbial oxidation of pyrite described in reactions Eqs. 1 and 2, respectively, are used to describe bioleaching.

$$FeS_2 + 14Fe^{3+} + 8H_2O \rightarrow 15Fe^{2+} + 2SO_4^{2-} + 16H^+ \quad (1)$$

$$4Fe^{2+} + O_2 + 4H^+ \rightarrow 4Fe^{3+} + 2H_2O \quad (2)$$

The indirect mechanism involves ferric ion attack of the ore particle at the surface containing FeS_2 (Eq. 1). In the acid-ferric leach step, 14 ferric ions are converted to the ferrous form as well as liberating an additional Fe center from the ore particle as ferrous. In such a mechanism, particle mass is lost to the solution, hence the particle surface area

Correspondence concerning this article should be addressed to R. Rawatlal at randhir.rawatlal@uct.ac.za.

will change with particle-solution contact time and is therefore a function of the particle residence time. The ferrous ions are restored to the ferric form by microbial action in the microbial oxidation step (Eq. 2). Therefore, the micro-organisms maintain the reaction environment at conditions that promote the liberation of ferrous ions from ore particles. The particle-solution dynamics involve the loss of particle mass due to reaction, and consequently the change in particle surface area with the particle residence time resulting from the two bioleaching subprocesses (Eqs. 1 and 2).

Numerous authors have attempted formulating the rate expression for reaction (1) in terms of exposed mineral surface area per unit mass of solution.[5–8] Since the focus in this article is reactor engineering rather than the kinetics, the simplest available kinetics will be used for model development. The kinetic rate expression proposed by McKibben and Barnes[5] (Eq. 3) is used.

$$-r''_{FeS_2} = k\left(\frac{C_{Fe^{3+}}}{C_{H^+}}\right)^{0.5} \tag{3}$$

where k is the intrinsic surface reaction rate constant [mol s^{-1} m^{-2}] and C_{Fe3+} and C_{H+} are the concentrations of the ferric ions and protons in solution [mol m^{-3}].

The microbial oxidation reaction rate is based on modified Michaelis-Menton and Monod-type kinetics,[9] and simplified by Hansford[10] (Eq. 4):

$$-r_{Fe^{2+}} = \frac{C_X q^{max}_{Fe^{2+}}}{1 + K\frac{C_{Fe^{3+}}}{C_{Fe^{2+}}}} \tag{4}$$

where $q^{max}_{Fe^{2+}} = 0.0019$ mol Fe^{2+} mol carbon^{-1} s^{-1} is the maximum microbial specific ferrous iron utilization rate, $K = 0.0005$ the inhibition constant, and C_x [mol m^{-3}] the concentration of the biomass which is obtained by dividing the rate of CO_2 consumed [mol m^{-3} s^{-1}] by the dilution rate [s^{-1}]. The microbial oxidation reaction rate constants were taken for the bioleaching of sulfide minerals in the presence of *Leptospirillum ferrooxidans*.[11]

A number of bioleach reactor models have been published, many of which focus on the biological aspects of the system (Eq. 2). However, they fail to consider the impact of acid-ferric leaching on the reactor performance (Eq. 1). One of the earliest models applied to tank bioleaching was proposed by Pinches et al.[3] The model assumed that biomass is proportional to the fractional conversion of pyrite.[3,12] The model was based only on microbial growth kinetics by means of the empirical logistic equation ignoring the effects of the acid-ferric leach kinetics or the change in ore particle size resulting from flow effects or from the leaching reaction. Similarly, the model proposed by Breed and Hansford[13] did not incorporate particle dynamics into the modeling process. The model was based on the assumption that the rate of ferrous iron production and consumption were equal at steady state. This assumption lead to the questionable conclusion that the chemical and microbial oxidation reactions were, at steady state, independent of the mineral sulfide (pyrite) concentration and therefore could be described by the rate of iron turnover via the solution redox potential (C_{Fe3+}/C_{Fe2+}).

The model introduced by Crundwell[12,14–16] incorporated the acid-ferric leach and microbial oxidation kinetics and utilized a distribution of mineral particle sizes to predict reactor performance by means of a population balance model (PBM). Brochot et al.[17] also proposed a PBM based on particle size distributions. The reduction in particle size was modeled by a first order kinetic rate, and was not based on the intrinsic kinetics from the generally accepted subprocess mechanism proposed by Boon et al.[18]

The model proposed by Crundwell[16] is limited to perfectly mixed systems at steady state. Given the scale of bioleach processes, such assumptions are unrealistic, and we seek in this article to uncouple these. The model developed in this article incorporates bio-oxidation kinetics, acid-ferric leach kinetics as well as the effect of particle size and age distributions on reactor performance using a modified PBM approach that requires the numerical solution of only a system of ODEs with well defined initial conditions, rather than boundary value problems.

Model Formulation

When developing the bioleach reactor model, the reactor bioleaching rate r^R and conversion X^R will be assumed to be the variables that determine reactor performance, and hence the objectives of the model formulation. The conversion X^R of pyrite ore to products is given by the relative difference between the inlet pyrite mass $\dot{M}^R_{inlet}$ [kg s^{-1}] and outlet pyrite mass $\dot{M}^R_{outlet}$ [kg s^{-1}] (Eq. 5).

$$X^R = 1 - \frac{\dot{M}^R_{outlet}}{\dot{M}^R_{inlet}} \tag{5}$$

The average rate of pyrite surface removal per unit mass of particle for a given size is defined as the particle leaching reaction rate r' [mol s^{-1} kg^{-1}]. The reaction rate can be described by the shrinking particle model.[19] As the reaction proceeds, the unreacted mineral particle is reduced in size while liberating mass into the aqueous phase. The available particle surface area then drops with increasing particle-solution exposure time.

The inlet and outlet mineral sulfide ore mass flowrates are not equal since the bioleaching reaction effectively transfers particle mass to the solution phase. From the continuity equation and applying the steady state assumption, the total rate of effluent pyrite ore mass will be equal to the rate of consumption of the inlet mass (Eq. 6).

$$\dot{M}^R_{outlet} = \dot{M}^R_{inlet} - r^R \mathrm{MM}_{FeS_2} V^R \tag{6}$$

where r^R [mol s^{-1} m^{-3}] is the reactor bioleaching rate, which is the overall reactor leaching rate (see the following section), MM_{FeS2} [kg mol^{-1}] the molar mass of pyrite, and V^R [m^3] the volume of the reactor. Since the intrinsic surface reaction rate r'' [mol s^{-1} m^{-2}] is area-based, the formulation of the reactor bioleaching rate r^R becomes complicated by the dependence of particle surface area on particle-reactor exposure time (residence time) and inlet particle size. Furthermore, there are distributions of reactor residence time

and particle size that complicate developing the reactor bioleaching rate r^{R}. The following sections develop the relationships among the rates r'', r', and r^{R}.

Particle Dynamics

If the rate at which particle mass is liberated into solution is due to particle-solution contact time, a relationship between the particle size and the particle age should be established.

If we consider a particle entering a reactor at time t_0 [s] and present at time t [s], the particle will have resided there $\theta = t - t_0$ time units.

Generally, the feedstream will have particles of various initial sizes l_0 [m]. In the case of spherical geometry, l_0 may be the initial particle diameter. The corresponding initial specific surface area A_0^{p} is then $\frac{\pi l_0^2}{M_0^{p}}$ [m^2 kg^{-1}] where M_0^{p} is the initial mass of the particle.

Assuming steady reaction conditions, the rate of change of particle mass will be the product of the intrinsic surface reaction rate r'' [mol s^{-1} m^{-2}], the particle surface area A [m^2], and molar mass MM_{FeS2} (Eq. 7). As particle mass is liberated into the solution phase due to reaction and solution contact time θ, the particle surface area $A(\theta)$ and hence the particle mass $M^{p}(\theta)$ are functions of the particle age.

$$\frac{dM^{p}}{d\theta} = -r''A(\theta)\mathrm{MM}_{\mathrm{FeS}_2} \tag{7}$$

The particle surface area is the product of the specific surface area and the particle mass $A(\theta) = A^{p}(\theta)M^{p}(\theta)$.

Assuming spherical particle geometry and constant particle density, the particle surface area and volume can be expressed in terms of size, and substituted into Eq. 7 to obtain a differential in particle size (Eqs. 8 and 9).

$$\frac{d}{d\theta}\left(\frac{\pi}{6}l^3\right) = \frac{r''}{\rho}\cdot \pi l^2 \cdot \mathrm{MM}_{\mathrm{FeS}_2} \tag{8}$$

By chain differentiation of the LHS of Eq. 8, the surface area term πl^2 cancels out resulting in Eq. 9.

$$\frac{dl}{d\theta} = \frac{-2r''}{\rho}\mathrm{MM}_{\mathrm{FeS}_2} \tag{9}$$

If the solution concentrations are constant with respect to time, then the intrinsic reaction rate is also constant, and as such Eq. 9 can be integrated over particle age $\theta' = [0; \theta]$ with initial condition $l(\theta = 0) = l_0$, to yield the relationship between the particle size and age (Eq. 10).

$$l(\theta) = l_0 - \left(\frac{2r''}{\rho}\mathrm{MM}_{\mathrm{FeS}_2}\right)\cdot\theta \tag{10}$$

Equation (10) reinforces that the particle size and hence the particle surface area is a function of age and initial size (Eq. 11). Similarly, since the particle leaching rate is the product of the intrinsic surface rate r'' with particle surface area $A(\theta, l_0)$, it follows that the particle leaching rate is also a function of age and size (Eq. 12).

$$A(\theta, l_0) = \pi l(\theta, l_0)^2 \tag{11}$$

$$r'(\theta, l_0) = r''A^{p}(\theta, l_0) \tag{12}$$

The particle mass M^{p} can be expressed as a function of the particle age and initial size $M^{p}(\theta, l_0)$ using Eq. 10 to obtain the conversion of a single particle X^{p} (Eq. 13).

$$X^{p}(\theta, l_0) = 1 - \left(\frac{l(\theta)}{l_0}\right)^3 \tag{13}$$

Figure 1 illustrates the dynamics of the particle conversion with the particle age θ [s] and initial size l_0 [m]. Equation (10) indicates the rate at which the particle size or mass decreases with age. Clearly, with an increase in particle age and a decrease in particle size, the particle conversion will increase. The conversion gradually reaches a maximum as the particle is consumed with age.

In this section the relationship amongst initial size, age, and rate was established for a single particle. Since the particle population in the reactor is distributed with respect to initial size and age, the overall reaction rate can only be predicted by accounting for contributions from all possible initial sizes and ages.

The following section will therefore establish the rate contribution of all particles in the reactor by defining the distribution of particles based on their initial size and age.

Reactor Model Formulation

In developing reactor age and size distribution, we consider a set of particles that enter the reactor at time t_0 with the size distribution $f_0(l_0)$ [m^{-1}], defined such that $f_0(l_0)\Delta l_0$ is the fraction of particles at the inlet in the size range $[l_0,\ l_0+\Delta l_0]$. The size distribution inside the reactor is $f(l)$ (Figure 2).

Furthermore, since a nontrivial distribution in age θ generally exists, we require the internal residence time distribution $I(\theta)$ defined such that $I(\theta)\Delta\theta$ is the fraction of particles in the reactor in the age range $[\theta,\ \theta+\Delta\theta]$.

When combining the particle size $f_0(l_0)$ and age $I(\theta)$ distributions with the particle dynamics through a complete segre-

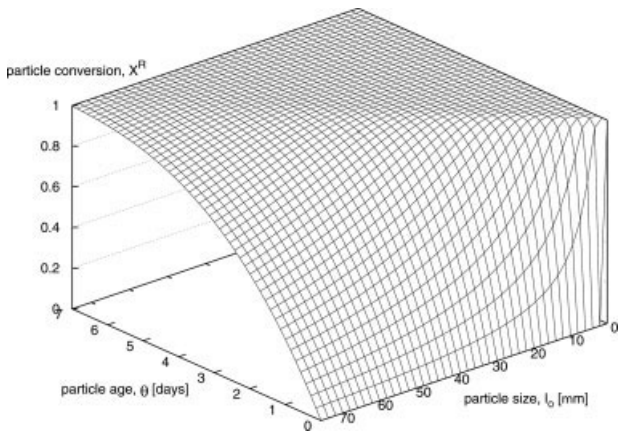

Figure 1. Plot of the particle conversion with particle age θ and initial size l_0.

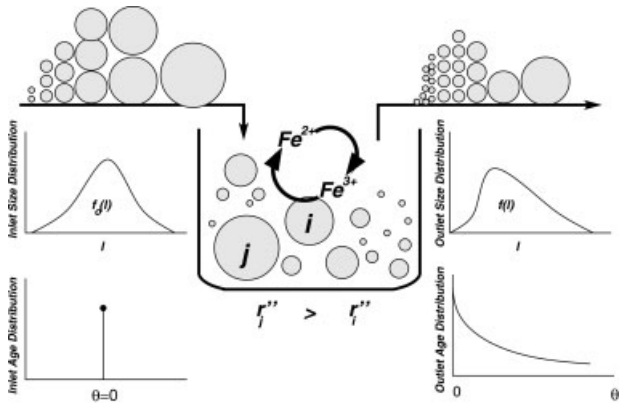

Figure 2. Model formulation for the overall reaction rate r^R in a bioleach reactor.

gation approach, the overall reactor bioleaching rate r^R [mol s^{-1} m^{-3}] can be predicted.

Macroscopic Balances

To determine the overall reactor performance, the solution and solid phase contributions to the overall reactor bioleaching rate need to be determined. The first step in modeling the reactor is therefore to write material balances for these phases. Assuming perfect mixing in each phase, species balances yield Eqs. 14 and 15.

Solution phase components

$$\frac{dC_i}{dt} = \frac{C_{\text{i,inlet}} - C_{i,\text{outlet}}}{\tau_{\text{solution}}} + \beta_i r^R + \gamma_i r_{Fe^{2+}} \tag{14}$$

Solid particle phase

$$\frac{dC_{FeS_2}}{dt} = \frac{C_{FeS_2,\text{inlet}} - C_{FeS_2,\text{outlet}}}{\tau_{\text{solid}}} + \beta_{FeS_2} r^R \tag{15}$$

where β_i and γ_i are the stoichiometric coefficients of species i for reactions 1 or 2, respectively and are assigned negative values for reactants and positive values for products. The first terms on the RHSs of the material balances (14) and (15), assuming perfect mixing, account for the flow of species into and out of the reactor, whereas the other RHS terms are the rates of change due to reaction(s).

Assuming uniform suspension of particles in the reactor, the mean residence times for the solid and solution phases will be equal $\tau_{\text{solid}} = \tau_{\text{solution}}$.

Since the solution phase is assumed perfectly mixed at the molecular level, the bio-oxidation rate r_{Fe2+} [mol s^{-1} m^{-3}] is the same at all points within the reactor. On the other hand, the concentration of pyrite varies from particle to particle, which complicates the estimation of the reactor bioleaching rate r^R. The objective in the following section will be to formulate the reactor bioleaching rate r^R.

The models developed can be distinguished by the initial size distribution used in predicting reactor performance. At the outset a trivial monosized particle feed, that remains the same size during the course of the reaction, is considered. This assumption is then progressively relaxed in the following models to one that considers an initial size distribution that undergoes a change in size due to reaction and particle solution contact time (Eq. 10). The models developed are then validated against pilot data obtained from Hansford and Miller[20] for a series of cascading tanks to determine the model's suitability for predicting reactor performance.

The following model developments are general and apply to all metal sulfides, hence the subscript FeS_2 will be replaced by MS.

Models

Model 1: Constant, uniform specific surface area

In Model 1 we consider monosized spherical particles that enter the bioleach reactor. It is assumed that all particles entering the reactor are of the same size, and will remain at this size in spite of leaching. The particle specific leaching rate r′ will therefore be the same for all particles in the reactor no matter what age they may have resided there. The particle specific leaching rate r' [mol s^{-1} kg^{-1}] is the product of the intrinsic surface reaction rate r″ [mol s^{-1} m^{-2}] and the particle specific surface area A_0^p [m^2 kg^{-1}] (Eq. 16).

$$r' = r'' A_0^p \tag{16}$$

The overall reactor bioleaching rate r^R may then be obtained as the product of the particle specific leaching rate r' and the constant total reactor solids mass as given by Eq. 17.

$$r^R = r' C_{\text{MS,inlet}} \text{MM}_{\text{MS}} \cdot \phi_{\text{MS}} \tag{17}$$

where $C_{\text{MS,inlet}}$ [mol m^{-3}] is the molar concentration of the mineral sulfide ore in the inlet stream into the reactor, MM_{MS} the molar mass of the pure mineral sulfide ore [kg mol^{-1}], and ϕ_{MS} the fraction of the pure mineral sulfide in the ore.

The overall reactor conversion X^R may then be obtained from the product of the overall reactor bioleaching rate r^R with the mean residence time relative to the inlet mineral sulfide ore concentration $C_{\text{MS,inlet}}$ (Eq. 18).

$$X^R = \frac{r^R \tau}{C_{\text{MS,inlet}}} \tag{18}$$

In this model, since the rate of dissolution and the mass of solids remain constant throughout the course of reaction, the conversion of the mineral sulfide particles X^R is directly proportional to the mean residence time.

The model was validated against pilot plant data for a cascade of stirred tanks in series.[20] The conversion predicted by the model was fitted to the measured conversions by adjusting only the acid-ferric leaching rate constant k (Eq. 3). The solution concentrations of each of the tanks were determined from the material balances (Eq. 14) and used as the inlet concentrations for the subsequent tank in the series.

Model validation with the pilot plant data shows the expected (see Eq. 18) linear increase of conversion with residence time for each tank (Figure 3). The pilot plant data shows that conversion changes with residence time and with different reactor configurations. This model, however, does

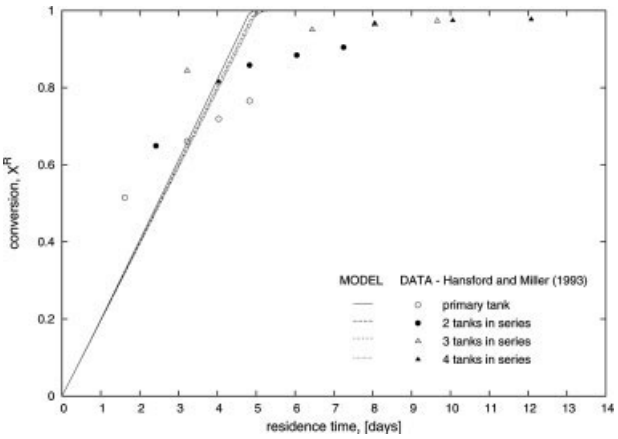

Figure 3. Reactor bioleaching conversion for Model 1 (constant specific surface area) vs. pilot plant data.[20]

not incorporate the effect of different reactor configurations on the overall conversion, making conversion independent of the number of reactors. The conversion for the reactors in the series is however dependent on the solution concentrations and thus the slope of the modeled conversion changes.

Clearly, the fit is rather poor, and the assumption of constant particle size must be relaxed. The following model incorporates age and hence surface area distributions.

Model 2: Age-dependent particle size distribution

In Model 2 the inlet stream to the reactor is assumed to contain particles of the same size that will be exposed to the solution phase in the reactor for different periods of time. The particle surface area A^{p} is therefore age dependent, resulting in a particle leaching rate r' [mol s^{-1} kg^{-1}] that varies from particle to particle (Eq. 19).

$$r'(\theta) = r'' A^{\mathrm{p}}(\theta) \tag{19}$$

where the intrinsic surface reaction rate r'' [mol s^{-1} m^{-2}] depends only on the solution concentrations.

Since $I(\theta)\Delta\theta$ is the fraction of particles in the age range [θ, $\theta+\Delta\theta$], the average particle leaching rate $\overline{r^{\mathrm{p}}}$ will be the sum of all rate contributions r' [mol s^{-1} kg^{-1}] in all particle fractions $I(\theta_i)\Delta\theta_i$ over age intervals [θ_i, $\theta_i+\Delta\theta_i$]. The overall reactor bioleaching rate r^{R} is therefore the product of the average particle leaching rate $\overline{r^{\mathrm{p}}}$ [mol s^{-1} m^{-3}] with the total number of particles N^{T} integrated over the age interval [0, ∞] (Eq. 20).

$$r^{\mathrm{R}} = \int_0^\infty r'(\theta)\frac{M^{\mathrm{p}}(\theta)}{V^{\mathrm{R}}}\phi_{\mathrm{MS}}N^{\mathrm{T}}I(\theta)d\theta \tag{20}$$

Model 2 was validated against the pilot plant data[20] using the simplifying assumption that the mean particle size from the preceding tank is the inlet particle size of all particles to the subsequent tank in the series. The conversion data points were fitted using the same method applied in Method 1 utilizing a RTD for a perfectly mixed reactor (Figure 4).

In contrast to Model 1, the pilot plant data and the model are in close agreement at low conversions, although the model's ability to predict reactor performance at higher conversions is limited.

While Model 2 is an improvement on Model 1, it still assumes uniform particle size in the feed stream whereas in reality the typical feed stream is not uniform. In the following model, the size restrictions applied in Models 1 and 2 are relaxed.

Model 3: Variable inlet particle size with age distribution in the reactor

In relaxing the single-size assumptions applied in Models 1 and 2, we now acknowledge that the inlet stream contains a nontrivial distribution in particle size. As in Model 2, a reactor age distribution is used.

With regard to the particle dynamics, larger particles will leach at a greater rate than smaller particles due to the larger availability of surface area, therefore the particles will leave the reactor with a different size distribution than upon entering the reactor. If perfect mixing is assumed, the particle age and size distributions within the reactor will be the same as in the outlet stream.

As the particle surface area is a function of the particle residence time and the inlet particle size, the particle leaching rate r' can be expressed as follows (Eq. 21):

$$r'(\theta, l_0) = r'' A^{\mathrm{p}}(\theta, l_0) \tag{21}$$

We assume that the inlet particle size distribution $f_0(l_0)$ is statistically independent of the reactor internal age distribution $I(\theta)$. The assumption of perfect mixing also implies that the particle size distribution inside the reactor must be the same at the exit, and hence the rate of exit of any particle does not depend on the particle size.

The product of the size and age fractions $f_0(l_0)\Delta l_0 I(\theta)\Delta\theta$ is therefore the fraction of particles in the age range [θ, $\theta+\Delta\theta$] and size range [l_0, $l_0+\Delta l_0$] in the reactor. Hence, the overall reaction rate can be determined using the segregation approach applied in Eq. 22.

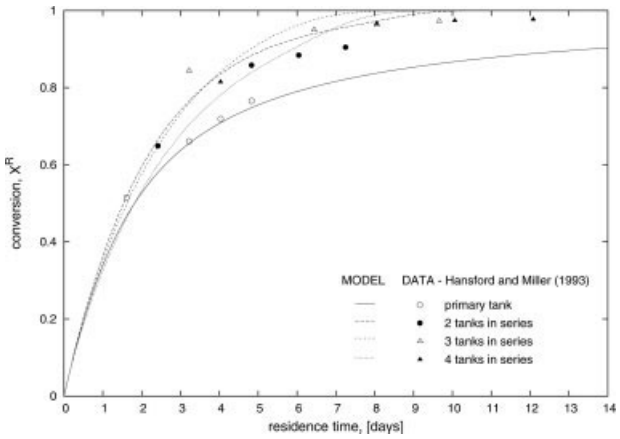

Figure 4. Reactor bioleaching conversion for Model 2 (monosized feed particles) vs. pilot plant data.[20]

$$\overline{r^{\mathrm{R}}} = \sum_{j}^{n} \sum_{i}^{m} r'(\theta_i, l_{0\mathrm{j}}) \frac{M_i^{\mathrm{p}}(\theta_i, l_{0j})}{V^{\mathrm{R}}} \phi_{\mathrm{MS}} I(\theta_i) \Delta\theta_i f_0(l_{0\mathrm{j}}) \Delta l_{0\mathrm{j}} \quad (22)$$

where Eq. 23 is the differential form of Eq. 22.

$$r^{\mathrm{R}} = \int_0^{\infty} \int_0^{\infty} r'(\theta, l_0) \frac{M^{\mathrm{p}}(\theta, l_0)}{V^{\mathrm{R}}} \phi_{\mathrm{MS}} N^{\mathrm{T}} I(\theta) f_0(l_0) d\theta dl_0 \quad (23)$$

Alternatively, the segregation model may be used to determine the overall conversion X^{R} in Eq. 24

$$X^{\mathrm{R}} = \int_0^{\infty} \int_0^{\infty} X^{\mathrm{p}}(\theta, l_0) f(l_0) I(\theta) d\theta dl_0 \quad (24)$$

where $X^{\mathrm{p}}(\theta, l_0)$ is the conversion of a single particle in terms of age and size as shown in Eq. 13.

The model simulation result was compared with plant data[20] and plotted in Figures 5 and 6 using the same validation method applied for Models 1 and 2, using the outlet size distribution from tank $n-1$ as the inlet size distribution for the subsequent tank n in the series $f_{0,n}(l_{0,n}) = f_{n-1}(l_{n-1})$.

A model that utilizes a RTD that only accounts for the distribution in total system age, for example a tanks-in-series RTD, is limited to predicting conditions for only the inlet stream to the first tank and the outlet stream from the last tank in the series assuming that the conditions over each reactor is constant. By considering each reactor independently using a perfectly mixed RTD for each tank in the series and noting that the particle size distribution entering subsequent tanks in the series change due to leaching, the conditions of each of the intermediate streams can be determined.

Since the mass fraction of particles $f_{0,n+1}(l_{0,n+1})\Delta l_{0,n+1}$ entering the subsequent tank is the relative mass difference of all particles M^{p} in the size range $[l_0,\ l_0+\Delta l_0]$, the inlet size distribution of particles in the following tank will be the inverse product of the total initial mass of all particles entering the tank and the differential in particle mass with the inlet particle size (Eq. 26)

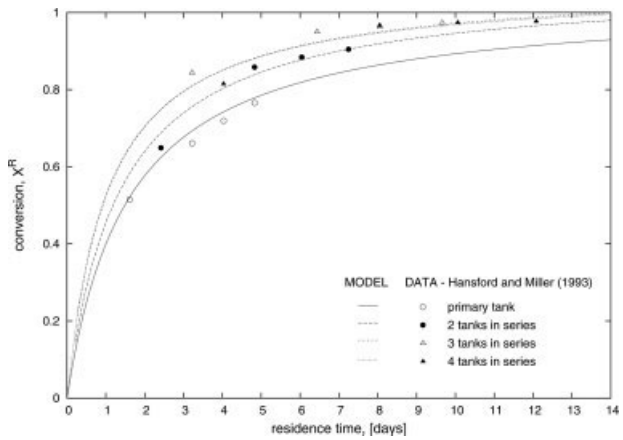

Figure 5. Reactor bioleaching conversion for Model 3 (age and size distributional effects) vs. pilot plant data.[20]

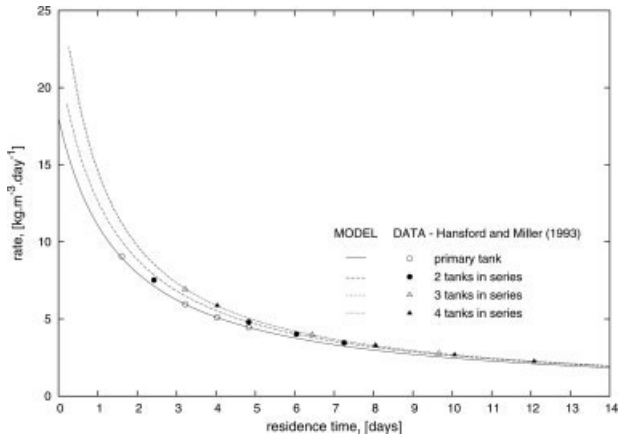

Figure 6. Overall reactor bioleaching rate for Model 3 (age and size distributional effects) vs. pilot plant data.[20]

$$f_n(l_n)\Delta l_n = \frac{M^{\mathrm{p}}(l_{0,n}) - M^{\mathrm{p}}(l_{0,\mathrm{n}} - \Delta l_{0,\mathrm{n}})}{M^{\mathrm{p}}_{\mathrm{total}}} \quad (25)$$

as such

$$f_{0,n+1}(l_{0,n+1}) = \frac{1}{\int_0^{\infty} \int_0^{\infty} M^{\mathrm{p}}(l_{0,n}) I(\theta) f_{0,n}(l_{0,n}) d\theta dl_0} \cdot \frac{dM^{\mathrm{p}}(l_{0,n})}{dl_{0,n}} \quad (26)$$

The average bioleaching reaction rate $\overline{r^{\mathrm{R}}}$ in each subsequent tank in the series is thus based on the outlet size distribution from the preceding tank $f_{0,n}(l_{0,n}) = f_{n-1}(l_{n-1})$ (Eq. 27)

$$\overline{r_n^{\mathrm{R}}} = \int_0^{\infty} \int_0^{\infty} r_n'(\theta, l_{0,n}) \frac{M_n^{\mathrm{p}}(\theta, l_{0,n})}{V_n^{\mathrm{R}}} \phi_{\mathrm{MS}} f_{0,n}(l_{0,\mathrm{n}}) I(\theta) d\theta dl_0 \quad (27)$$

Figure 5 indicates the expected increasing trend in conversion with residence time. With an increase in the number of tanks the conversion increases for the same mean residence time. This is to be expected since more efficient use of reactor volume is made and therefore a higher conversion is achieved as compared to a single tank (Figure 5).

The model was further compared with the average bioleaching reactor rate for each tank in the series. From Figure 6 it is clear that the model, which is a function of the age and initial size distribution, is able to predict the rates at each mean residence time.

The model's ability to predict the pilot plant data is greatly improved over Models 1 and 2. In contrast to Model 2, Model 3 is able to achieve good agreement with the data at both high and low conversions.

Future Model Extensions

In contrast to previous PBMs presented in the literature (Crundwell,[18] Brochot et al.[17]), the model presented here explicitly describes the overall reaction rate r^{R} or the overall

conversion X^R in the reactor as a function of the age distribution $I(\theta)$. It is therefore a trivial exercise to now incorporate the recently available advances in residence time distribution theory, in particular the unsteady state solution.[21]

The application of the present model can therefore be extended to the case in which the particle flowrate is changing with time by incorporating the unsteady state solution to residence time distribution for perfectly mixed vessels given in Eq. 28.[21]

$$I(t,\theta) = \frac{h_{in}(t-\theta)}{H(t)} \exp\left(-\int_{t-\theta}^{t} \frac{h_{out}(t')dt'}{H(t')}\right) \tag{28}$$

where $I(t,\theta)$ is defined such that $I(t,\theta)\Delta\theta$ is fraction of particles in the reactor at time t in age range $[\theta, \theta+\Delta\theta]$, $h_{in}(t)$ and $h_{out}(t)$ are the time-dependent entry and exit flowrates to and from the reactor respectively, and $H(t)$ is the particle holdup in the reactor.

Reactors in series may also be modeled using the results from the same article by application of the joint residence time distribution function $\rho_i(t,\theta)$, $i \leq N$, defined such that the product $\rho_i(t,\theta)\prod_{j=1}^{i}\Delta\theta_j$ represents the fraction of particles residing in reactor i at time t identified by the age range $[\theta_i, \theta_i+\Delta\theta_i]$, which previously occupied vessels 1, 2, ..., $i-1$ for $[\theta_1, \theta_1+\Delta\theta_1]$, $[\theta_2, \theta_2+\Delta\theta_2]$, ..., $[\theta_{i-1}, \theta_{i-1}+\Delta\theta_{i-1}]$ periods of time, respectively. For the case of CSTRs in series, the following solution given by Eq. 29 may be applied.

$$\rho_N(t,\theta) = \frac{\exp\left(\sum_{i=1}^{N}\left[\alpha_j(t_{0,j+1}) - \alpha_j(t_{0,j})\right]\right)}{\prod_{i=1}^{N}\tau_i'(t,\theta)} \tag{29}$$

with

$$\begin{aligned}\tau'(t,\theta) &= \left[\tau_1'(t,\theta), \tau_2'(t,\theta), ..., \tau_{N-1}'(t,\theta), \tau_N'(t,\theta)\right] \\ &= \left[\tau_1(t_{0,2}), \tau_2(t_{0,3}), ..., \tau_{N-1}(t_{0,N-2}), \frac{H_N(t)}{h_1(t_{0,1})}\right]\end{aligned}$$

where $\tau_i(t)$ is the inlet-flow based mean residence time in the ith reactor at time t, and $\alpha_i(t) = -\int_0^t \frac{dt'}{\tau_i(t')}$ the average ratio of real time to mean residence time.

In addition to modeling unsteady state flow, the explicit dependence on the internal RTD shown in the final solution also makes it possible to predict the performance of imperfectly mixed reactors if the RTD for such reactor has been measured.

Conclusions

Presently, PBMs focus on the size of the particle ignoring the effect of particle residence time on the overall reactor performance. However, in tank bioleaching the particles within the reactor remain in contact with the solution phase for different periods of time indicating that the particle age should also have a significant contribution to the overall reaction rate. The objective of this article was therefore to verify which reactor parameters are necessary to fully describe the dissolution of mineral sulfide particles in the bioleaching process.

Bioleach reactor models were derived from first principles incorporating material balances with acid-ferric leaching and microbial oxidation kinetics. The reactor performance was initially modeled by applying the most restrictive assumptions that did not consider the age or size of the particles in solution. These assumptions were relaxed by first introducing the age distribution of equally sized particles in solution and thereafter the bioleaching of particles of nontrivial inlet size distribution were considered.

Of the three models presented, the third model is the most general. Comparing the pilot plant data with the three models, it was found that the third model, which uses the least restrictive assumptions, is able to predict the reactor performance with the greatest accuracy. The improved predictive capabilities of Model 3 over the preceding models, indicates that both the age and size contributions of all particles in the reactor are necessary to fully describe the reactor performance in tank bioleaching. Further, Model 3 in this study has uncoupled the variation of particle size with time to explicitly consider a distribution in particle age in the reactor. This explicit dependence allows for the model to be extended to unsteady state behavior and imperfect mixing.

Acknowledgments

This work was carried out in the frame of BioMinE (European project contract NMP1-CT-500329-1). The authors acknowledge the financial support given to this project by the European Commission under the Sixth Framework Program for Research and Development. The authors also wish to thank their various partners on the project for their contributions to the work reported in this paper.

Notation

Greek letters

α_i = average ratio of real time to mean residence time
β_i = stoichiometric coefficient of species i for reaction (1)
γ_i = stoichiometric coefficient of species i for reaction (2)
θ = age of a particle [s]
$\rho_N(t, \theta)$ = joint residence time distribution function for N tanks [s^{-N}]
τ = reactor residence time [s]
$\tau_i(t)$ = inlet-flow based mean residence time in the ith reactor at time t
ϕ_{MS} = fraction of the pure mineral sulfide in the ore

Latin symbols

A^p = specific surface area of a particle [m^2 kg^{-1}]
C_{Fe2+} = concentration of ferrous ions [mol m^{-3}]
C_{Fe3+} = concentration of ferric ions [mol m^{-3}]
C_{H+} = concentration of protons [mol m^{-3}]
C_{MS} = concentration of the mineral sulfide ore [mol m^{-3}]
C_x = concentration of biomass [mol m^{-3}]
$f_0(l_0)$ = the normal distribution representing the probability of particles in a specific size range [m^{-1}]
$h_{in}(t)$ = time-dependent entry flowrate to the reactor [kg s^{-1}]
$h_{out}(t)$ = time-dependent exit flowrate from the reactor [kg s^{-1}]
$H(t)$ = particle holdup in the reactor [kg]
$I(\theta)$ = the internal age distribution of particles [s^{-1}]
$I(t,\theta)$ = the unsteady state internal age distribution of particles [s^{-1}]
k = intrinsic surface reaction rate constant [mol s^{-1} m^{-2}]
K = inhibition constant
l_0 = initial particle size or diameter [m]
MM_{FeS2} = molar mass of pyrite ore particle [kg mol^{-1}]
MM_{MS} = molar mass of the pure mineral sulfide ore [kg mol^{-1}]

M^{p} = mass of a single particle [kg]
M^{R} = total mass of all particles in the reactor [kg]
n = tank number
N = the total number of tanks
N^{T} = the total number of particles in the reactor
$q^{\max}_{\mathrm{Fe}^{2+}}$ = maximum microbial specific ferrous iron utilization rate [mol Fe^{2+} mol carbon^{-1} s^{-1}]
r'' = intrinsic surface reaction rate [mol s^{-1} m^{-2}]
r' = particle leaching rate [mol s^{-1} kg^{-1}]
$\overline{r^{\mathrm{p}}}$ = average particle leaching rate [mol s^{-1} m^{-3}]
$\overline{r^{\mathrm{R}}}$ = average reactor bioleaching rate [mol s^{-1} m^{-3}]
r^{R} = reactor bioleaching rate [mol s^{-1} m^{-3}]
$r_{\mathrm{Fe2+}}$ = bio-oxidation rate [mol s^{-1} m^{-3}]
V^{R} = reactor volume [m^3]
X^{p} = particle conversion
X^{R} = reactor bioleaching conversion

Literature Cited

1. Acevedo F. The use of reactors in biomining processes. *Electron J Biotechnol*. 2000;3:184–194.
2. Olson GJ, Brierley JA, Brierley CL. Bioleaching review part B: progress in bioleaching—applications of microbial process by the minerals industries. *Appl Microbiol Biotechnol*. 2003;63:249–257.
3. Pinches A, Chapman JT, te Riele WAM, van Staden M. The performance of bacterial leach reactors for the preoxidation of refactory gold bearing sulphide concentrates. In: Norris PR, Kelly DP, editors. *Biohydrometallurgy, Proc. Int. Symp*. Warwick, STL, Kew, Surrey, UK, 1987:329–344.
4. Dew DW, Lawson EN, Broadhurst JL. The BIOX® process for bio-oxidation of gold-bearing ores or concentrates. In: Rawlings DE, editor. *Biomining: Theory, Microbes and Industrial Processes*. Berlin: Springer, 1997:45–61.
5. McKibben MA, Barnes HL. Oxidation of pyrite in low temperature acidic solutions: rate laws and surface textures. *Geochim Cosmochim Acta*. 1986;50:1509–1520.
6. Rimstidt JD, Newcom WD. Measurement and analysis of rate data: the rate of reaction of ferric iron with pyrite. *Geochim Cosmochim Acta*. 1993;57:1919–1934.
7. Williamson MA, Rimstidt JD. The kinetics and electrochemical rate-determining step of aqueous pyrite oxidation. *Geochim Cosmochim Acta*. 1994;58:5443–5454.
8. May N, Ralph DE, Hansford GS. Dynamic redox potential measurement for determining the ferric leach kinetics of pyrite. *Miner Eng*. 1997;10:1279–1290.
9. Nemati M, Webb C. A kinetic model for biological oxidation of ferrous iron by *Thiobacillus ferrooxidans*. *Biotechnol Bioeng*. 1997;53:478–486.
10. Hansford GS. Recent developments in modelling the kinetics of bioleaching. In: Rawlings DE, editor. *Biomining: Theory, Microbes and Industrial Processes*. Berlin: Springer, 1997:153–176.
11. Boon M, Heijnen JJ. Chemical oxidation kinetics of pyrite in bioleaching processes. *Hydrometallurgy*. 1997;48:27–41.
12. Crundwell FK. Mathematical modelling of batch and continuous bacterial leaching. *Chem Eng J*. 1994;54:207–220.
13. Breed AW, Hansford GS. Modeling continuous bioleach reactors. *Biotechnol Bioeng*. 1999;64:671–677.
14. Crundwell FK. Progress in the mathematical modelling of leaching reactors. *Hydrometallurgy*. 1995;39:321–335.
15. Crundwell FK. Modelling, simulation and optimization of bacterial leaching reactors. *Biotechnol Bioeng*. 2001;71:257–265.
16. Crundwell F. The leaching number: its definition and use in determining the performance of leaching reactors and autoclaves. *Miner Eng*. 2005;18:1315–1324.
17. Brochot S, Durance MV, Villeneuve J, d'Hugues P, Mugabi M. Modelling of the bioleaching of sulphide ores: application for the simulation of the bioleaching/gravity section of the Kassese Cobalt Company Ltd process plant. *Miner Eng*. 2004;17:253–260.
18. Boon M, Hansford GS, Heijnen JJ. The role of bacterial ferrous iron oxidation in the bio-oxidation of pyrite. In: Vargas T, Jerez CA, Wiertz JV, Toledo H, editors. *Biohydrometallurgical Processing 1*. University of Chile: Santiago, 1995:153–163.
19. Yagi S, Kunii D. Fluidized-solids reactors with continuous solids feed. I. Residence time of particles in fluidized beds. *Chem Eng Sci*. 1961;16:354–380.
20. Hansford GS, Miller DM. Biooxidation of a gold-bearing pyrite-arsenopyrite concentrate. *FEMS MicrobiolRev*. 1993;11:175–182.
21. Rawatlal R, Starzak M. Unsteady-state residence-time distribution in perfectly mixed vessels. *AIChE J*. 2003;49:471–484.

Manuscript received Dec. 13, 2007, and revision received Feb. 12, 2008.